



# Enhanced photocatalytic activity of new photocatalyst Ag/AgCl/ZnO

Yuanguo Xu<sup>a,b</sup>, Hui Xu<sup>b</sup>, Huaming Li<sup>a,\*</sup>, Jiexiang Xia<sup>a</sup>, Chengtang Liu<sup>a</sup>, Ling Liu<sup>a</sup>

<sup>a</sup> School of Chemistry and Chemical Engineering, Jiangsu University, Zhenjiang 212013, PR China

<sup>b</sup> School of the Environment, Jiangsu University, Zhenjiang 212013, PR China

## ARTICLE INFO

### Article history:

Received 5 August 2010

Received in revised form

26 November 2010

Accepted 30 November 2010

Available online 8 December 2010

### Keywords:

Ag/AgCl/ZnO

Photocatalyst

Methyl orange

Noble metal

## ABSTRACT

A new composite photocatalyst Ag/AgCl/ZnO was fabricated by a two-step synthesis method under the hydrothermal condition. The sample was characterized by XRD, TG-DSC, SEM, TEM, DRS and XPS. The results showed that the samples were composed of Ag, AgCl and ZnO, and the particle size was in the range of 100 nm–1 μm. Methyl orange (MO) was used as a representative dye pollutant to evaluate the photocatalytic activity of Ag/AgCl/ZnO. The photocatalytic activity of Ag/AgCl/ZnO catalyst was higher than that of the pure ZnO catalyst. It was found that the Ag/AgCl/ZnO structure changed to Ag/ZnO gradually after several repeated experiments. However, the photocatalytic ability of the sample was not reduced. Finally, a possible photocatalytic mechanism was proposed.

© 2010 Elsevier B.V. All rights reserved.

## 1. Introduction

In the past decades, environmental problems have been increasingly serious with the development of the industry and economy of human society. It has provided the impetus to sustained fundamental and applied research in the aspect of environmental remediation. Various photocatalysts have been synthesized and studied, such as TiO<sub>2</sub> [1], ZnO [2], BiVO<sub>4</sub> [3], AgNbO<sub>3</sub> [4], ZnWO<sub>4</sub> [5], etc. ZnO, as a wide direct band gap (3.2 eV) semiconductor, has been attracting much attention in the past decades, and it has been used in different areas, such as solar cell [6], sensor [7,8], magnetic material [9], photoluminescence material [10] and photodegradation [11], etc. ZnO is a good photocatalyst, which presents higher photocatalytic activity than TiO<sub>2</sub> in the photodegradation of some organic compounds [12], so it is a suitable alternative of TiO<sub>2</sub>. However, the photocatalytic ability of the sample is still not high enough, because the low separating efficiency of the photoelectron–hole pairs for the single semiconductors seriously impedes the photocatalytic degradation efficiency of the pollutants. Besides, the structure of the ZnO crystal would be destroyed after consecutive use due to the photocorrosion effect [13]. In order to solve these drawbacks, a lot of efforts have been made to improve the photocatalytic activity of the pure ZnO semiconductor, such as the synthesis of different morphologies of ZnO [14], which has been proved to be more efficient in photocatalysis; semiconductor com-

bination (such as ZnO/In<sub>2</sub>O<sub>3</sub> [15], ZnO/TiO<sub>2</sub> [16], ZnO/SnO<sub>2</sub> [17], etc.); transition metals doping [18]; rare-earth metals loading [19] and noble metal deposition [20–22]. It has been proved that among these methods, the modification with noble metal is an effective way to improve the separation of photo-generated electron–hole pairs.

And recently, Ag/AgX [23] (X=Cl, Br) structure has been reported as an efficient photocatalyst, which was named as plasmonic photocatalyst [24]. Ag/AgX is a stable structure, and it has the property to act as the co-catalyst. A few of correlative photocatalysts have been synthesized, such as Ag/AgCl/TiO<sub>2</sub> [25], Ag/AgBr/WO<sub>3</sub>·H<sub>2</sub>O [26], and they are stable and efficient in degradation of the organic dye. The addition of Ag/AgX does enhance the photocatalytic ability of the catalysts. The results indicate that Ag/AgX is not only a good photocatalyst, but also a good co-catalyst.

Based on the above analysis, Ag/AgX as a cocatalyst could enhance the separation of electron–hole, thus the photocatalytic activity of the semiconductor increased. It can be inferred that Ag/AgCl/ZnO can be a potential candidate for photocatalysis, and Ag/AgCl/ZnO has not been reported ever before. This expectation led us to prepare a new photocatalyst Ag/AgCl/ZnO by a two-step hydrothermal method. And methyl orange (MO) aqueous solution was chosen as the model compound to estimate the photoactivity of the samples. The experimental result showed that the loading of a small amount of Ag/AgCl could enhance the photocatalytic ability of ZnO. The relationship between the photocatalytic activity and the structural features of the prepared catalysts was investigated through a systematic characterization analysis, and a possible mechanism of the reaction was proposed.

\* Corresponding author. Tel.: +86 511 88791800; fax: +86 511 88791708.  
E-mail address: [lihm@ujs.edu.cn](mailto:lihm@ujs.edu.cn) (H. Li).

## 2. Experimental

### 2.1. Material and sample preparation

All chemicals were analytical grade and used as received without purification. The ionic liquid [Bmim]Cl (1-butyl-3-methylimidazolium chloride) (99%) was purchased from Shanghai Chengjie Chemical Co. LTD.

### 2.2. Synthesis of ZnO

ZnO was prepared by a simple hydrothermal reaction. 12 mmol  $\text{Zn}(\text{CH}_3\text{COO})_2$  was dissolved into 30 ml distilled  $\text{H}_2\text{O}$ , and the aqueous solution was dripped into another solution which contained 30 ml distilled  $\text{H}_2\text{O}$  and 48 mmol NaOH. After being stirred at room temperature for 20 min, the reaction mixtures were transferred into a 100 ml Teflon-lined stainless steel autoclave, and then the autoclave was sealed and heated in an oven up to  $140^\circ\text{C}$ . The temperature was maintained for 24 h. When the reaction was completed, the autoclave was cooled to room temperature naturally. The obtained white precipitate was collected by centrifugation. Finally, it was dried in the air at  $50^\circ\text{C}$  for 8 h after being washed by water and alcohol.

### 2.3. Synthesis of the photocatalyst Ag/AgCl/ZnO

0.244 g (3 mmol) of the as-prepared ZnO was put into 5 ml distilled  $\text{H}_2\text{O}$ , and the mixture was stirred through the reaction. After 10 min, 5 ml EG was poured into the mixture. And then,  $\text{AgNO}_3$  was dissolved into 5 ml  $\text{H}_2\text{O}$  and dripped to the above solution ( $\text{Ag}:\text{ZnO} = 0.05:1$ , in molar ratio). Different molar ratios of Ag:ZnO (5, 20 and 40) were prepared and named as 5 at%, 20 at%, 40 at%. After 1 h, 0.985 g 1-butyl-3-methylimidazolium chloride ([Bmim]Cl) was added to the mixture, and stirred for 10 min. Finally, the solution was transferred into a 25 ml Teflon-lined stainless steel autoclave, and the autoclave was sealed and heated in an oven up to  $140^\circ\text{C}$ .

### 2.4. Characterization

X-ray diffraction (XRD) patterns of the samples were measured by X-ray diffractometer (Bruker D8) with  $\text{Cu K}\alpha$  radiation ( $\lambda = 1.54 \text{ \AA}$ ) in the range of  $2\theta = 20^\circ$ – $80^\circ$ , and the scan rate of XRD was  $6^\circ/\text{min}$ . Scanning electron microscopy (SEM) micrographs were observed by a FE-SEM (JEOL JSM-7001F). The diffuse reflectance spectra (DRS) were measured by UV–vis spectrometer (Shimadzu UV-2450). The X-ray photoelectron spectroscopy (XPS) was observed by VG MultiLab 2000. Thermogravimetry, differential scanning calorimetry, (TG-DSC) was done on STA-449C Jupiter (NET-ZSCH Corporation, Germany). Transmission electron microscopy (TEM) micrographs were taken with a JEOL-JEM-2010 (JEOL, Japan) operating at 200 kV.

### 2.5. Photocatalytic activity

The photocatalytic activity of ZnO and Ag/AgCl/ZnO was measured by the degradation of MO solution under the UV illumination (250 W). The reaction was carried out with 0.05 g photocatalyst suspended in 100 ml MO solution. The initial concentration of the MO solution was 10 mg/L. Before the UV lamps were turned on to start illumination, the solution was stirred for 0.5 h in dark to establish the adsorption/desorption equilibrium between the photocatalysts and the dyes. The solution was sampled at 10 min intervals and centrifuged to discard any sediment, and then monitored by UV–vis spectroscopy.

## 3. Results and discussion

### 3.1. XRD and SEM

Fig. 1 shows the XRD patterns of the photocatalysts ZnO, AgCl/ZnO and Ag/AgCl/ZnO with different molar ratios of Ag content. The inset displays the diffraction peak (at  $2\theta = 38.1^\circ$ ) assigned to metal Ag. In Fig. 1a, all patterns match very well with the JCPDS standard data of wurtzite ZnO (JCPDS cards nos. 36–1451). The peaks at  $2\theta = 31.8^\circ$ ,  $34.4^\circ$ ,  $36.3^\circ$ ,  $47.5^\circ$ ,  $56.6^\circ$ ,  $62.9^\circ$ ,  $66.4^\circ$ ,  $68.0^\circ$ ,  $69.1^\circ$ ,  $72.6^\circ$  and  $77.0^\circ$ , which are marked with “#”, are assigned to the (100), (002), (101), (102), (110), (103), (200), (112), (201), (004) and (202) planes of ZnO, respectively. In Fig. 1c, it is found that the XRD patterns of Ag/AgCl/ZnO are composed of ZnO, Ag and AgCl phases, and match their standard JCPDS cards nos. 36–1451, 04–0783 and 31–1238, respectively. The peaks at  $2\theta = 27.82^\circ$ ,  $32.24^\circ$ ,  $46.25^\circ$ ,  $54.81^\circ$ ,  $57.56^\circ$ ,  $67.4^\circ$ ,  $74.5^\circ$  and  $76.6^\circ$ , which are marked with “●”, are assigned to the (111), (200), (220), (311), (222), (400), (331) and (420) planes of cubic phase of AgCl crystal. The peaks at  $38.1^\circ$  and  $44.3^\circ$ , which are marked with “◆”, are assigned to the (111), and (200) planes of metallic

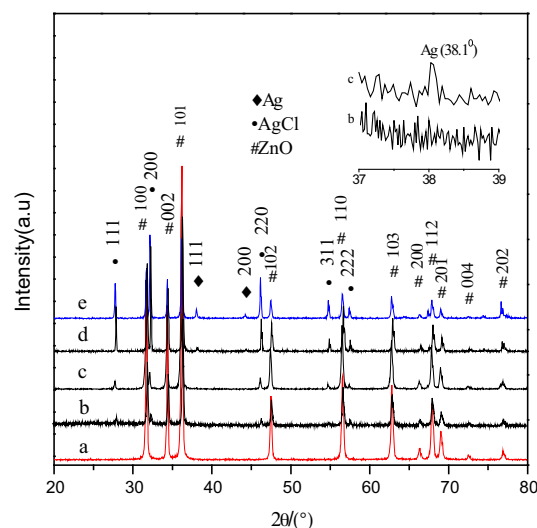


Fig. 1. XRD of the samples (a) ZnO (b) AgCl/ZnO (5 at%) (c) Ag/AgCl/ZnO (5 at%) (d) Ag/AgCl/ZnO (20 at%) (e) Ag/AgCl/ZnO (40 at%). The inset shows peaks of  $\text{Ag}^0$  in the AgCl/ZnO and Ag/AgCl/ZnO system.

Ag. The lattice parameters of ZnO are  $a = 3.25359 \text{ \AA}$ ,  $b = 3.25359 \text{ \AA}$ ,  $c = 5.21168 \text{ \AA}$ . The lattice parameters of the ZnO in the Ag/AgCl/ZnO material are  $a = 3.25561 \text{ \AA}$ ,  $b = 3.25561 \text{ \AA}$ ,  $c = 5.21545 \text{ \AA}$ . Negligible changes of all diffraction peak positions and lattice parameters of ZnO in the Ag/AgCl/ZnO samples were observed. It indicates that Ag/AgCl loading should be merely placed on the surface of the crystals without covalently anchored into the crystal lattice [27]. The diffraction peak (at  $2\theta = 38.1^\circ$ ) assigned to metal Ag is also displayed in the nanojunction system (the inset of Fig. 1). It indicates that the Ag/AgCl/ZnO has a peak at  $38.1^\circ$ , while the AgCl/ZnO does not have (Fig. 1b). It confirms that  $\text{Ag}^0$  existing in the Ag/AgCl/ZnO sample, and there is no  $\text{Ag}^0$  exists in the AgCl/ZnO sample. Because the deposit amount of Ag is very small, the peak of the  $\text{Ag}^0$  is weak. When the deposit amount of Ag is raised (Fig. 1 d and e), it can be clearly seen that the Ag peaks become obvious ( $2\theta = 38.1^\circ$ ).

Fig. 2 shows the SEM images of the (A) ZnO (B) Ag/AgCl/ZnO (5 at%) (C) Ag/AgCl/ZnO (40 at%) and (D) The EDS of the selected area of (C). The images clearly reveal that the samples are composed of small particles and nano-rod, and the lengths of the samples are in the range of 100 nm–1  $\mu\text{m}$ . It can be seen that the morphology and the size of the photocatalysts do not show significant changes after deposition of Ag/AgCl. The EDS analysis reveals that Ag and Cl elements were detected in the samples. According to the XRD results, it could be deduced that Ag/AgCl was deposited on the walls of ZnO.

### 3.2. TG-DSC

The thermal decomposition of Ag/AgCl/ZnO product was determined by thermogravimetric analysis (TG) under a  $\text{N}_2$  atmosphere. The TG curve (weight loss of samples in relation to the temperature of thermal degradation) is presented in Fig. 3. When the temperature is raised to  $800^\circ\text{C}$ , the weight decreased probably due to the evaporation of the gas, which had been adsorbed to the surface of ZnO powder. The loss of the weight is less than 0.5%. It could be concluded that the sample is of thermal stability under this temperature. No obvious peaks appear in the DSC curves of the Ag/AgCl/ZnO sample. It indicates that there is no obvious phase transition when the sample is treated at a high temperature.

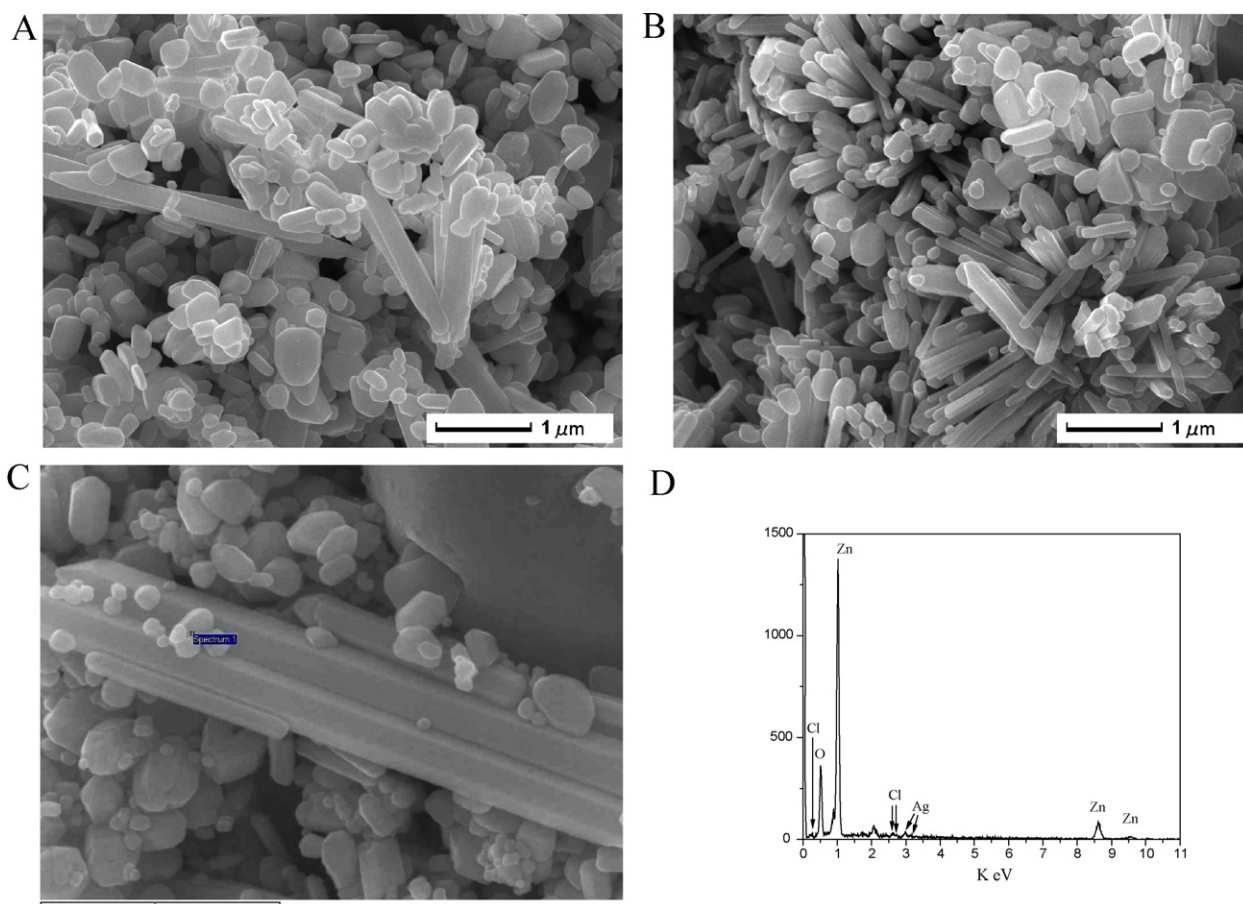


Fig. 2. SEM of the samples (A) ZnO (B) Ag/AgCl/ZnO (5 at%) and (C) Ag/AgCl/ZnO (40 at%) and (D) The EDS of the selected area of (C).

### 3.3. XPS analysis

The surface components and chemical states of Ag/AgCl/ZnO have been investigated by XPS analysis, and the corresponding experimental results are shown in Fig. 4. As shown in Fig. 4a, all of the peaks can be ascribed to Ag, Cl, Zn, O, and C elements and no peaks of other elements are observed. The appearance of C peak is mainly due to the adventitious hydrocarbon from the XPS instrument itself. Hence, it could be concluded that the samples are composed of Zn, O, Ag, and Cl, which are well consistent with the XRD results. Fig. 4 b–d show the high-resolution XPS spectra of Zn 2p, Ag 3d and Cl 2p in the Ag/AgCl/ZnO composite, respectively. The position of Zn 2p peak for the sample is at the value of 1021.8 eV,

which confirms that in the sample Zn element exists in the form of  $\text{Zn}^{2+}$ . Fig. 4c shows that Ag 3d peak appears at a binding energy of 366.8 eV. It shows that the peak shifts obviously to lower binding energy in comparison with the standard value of bulk Ag (368.2 eV) and the Ag 3d in Ag/ZnO catalyst (367.2 eV). It indicates that the shift of the binding energy of Ag 3d is primarily attributed to the interaction among the Ag, AgCl and ZnO [28–30]. Fig. 4d shows the spectra of Cl 2p. The binding energy of Cl 2p is at 198.4 eV, which confirms the Cl element exists mainly in the form of  $\text{Cl}^-$ .

### 3.4. DRS

Fig. 5 shows the DRS of ZnO and Ag/AgCl/ZnO. The Ag/AgCl/ZnO sample has much stronger absorption than the ZnO sample in the visible region, because Ag particles strongly absorb the light. It suggested that the photocatalytic property of Ag/AgCl/ZnO should be better than ZnO. The estimated value of the band gap ( $E_g$ ) of the samples could be calculated by the following formula [31]:

$$A = \frac{C(h\nu - E_g)^{n/2}}{h\nu}$$

Where  $A$ ,  $\nu$ ,  $E_g$ , and  $C$  are absorption coefficient, the light frequency, the band gap, and proportionality constant, respectively. According to the reference, the value of  $n$  for ZnO and Ag/AgCl/ZnO is 1. The  $E_g$  of ZnO and Ag/AgCl/ZnO are 3.224 eV and 3.225 eV (see the inset in Fig. 5), respectively. The little change of the  $E_g$  of the samples also explains why the catalysts do not show high activity under the visible light.

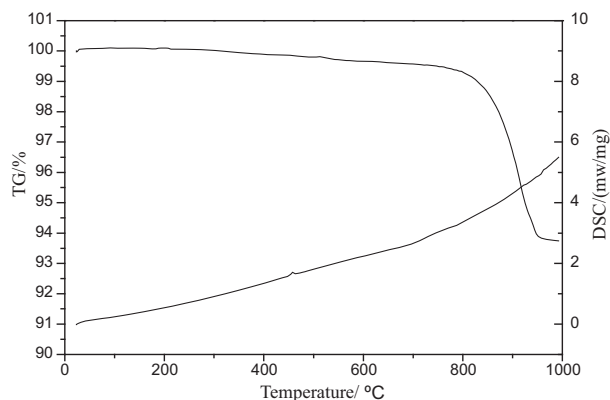


Fig. 3. TG-DSC of the Ag/AgCl/ZnO photocatalysts.

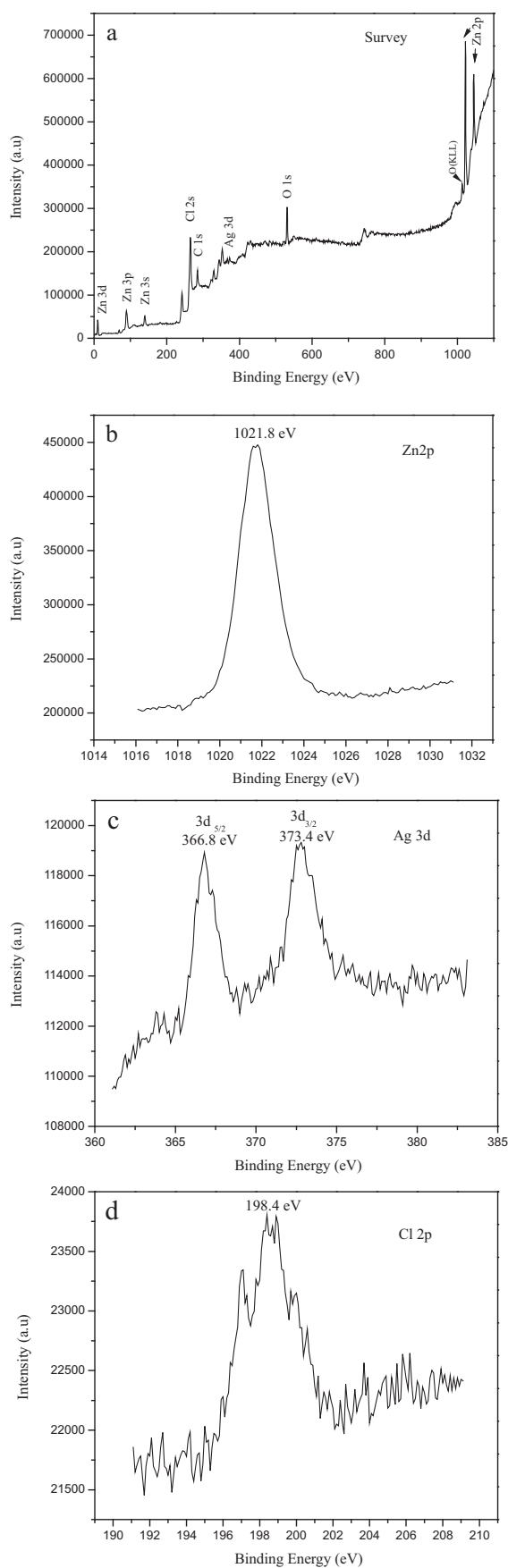


Fig. 4. XPS spectra of (a) survey spectrum of Ag/AgCl/ZnO (b) Zn 2p (c) Ag 3d and (d) Cl 2p.

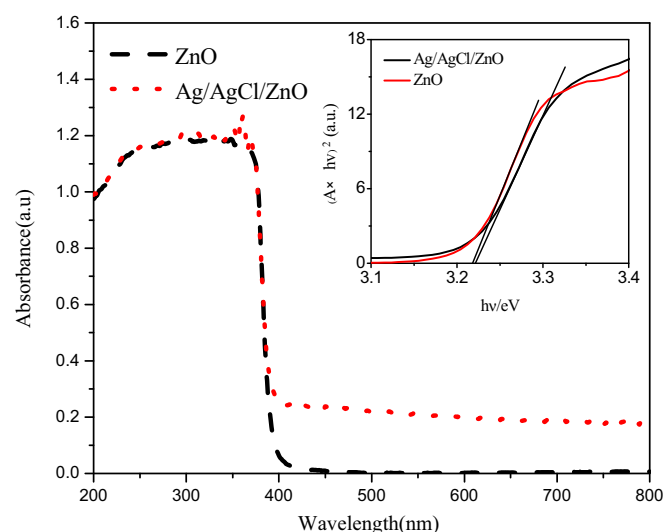


Fig. 5. DRS spectra of pure ZnO and Ag/AgCl/ZnO.

### 3.5. Photocatalytic Activity

The photocatalytic activity of the samples is shown in Fig. 6. It is found that the degradation efficiency of MO without photocatalysts is low, as shown in Fig. 6a. It suggests that the photoinduced self-sensitized photolysis of MO could be neglected. However, the concentration of the MO decreases rapidly with the addition of any catalysts. The pure ZnO shows activity in photocatalytic of MO, and the degradation efficiency of MO solution is 63% in 40 min. After loading Ag/AgCl, the degradation efficiency of the sample increases to 100% in 40 min. As a noble metal deposit catalyst, it has some improved characteristic when compared to the oxide deposit catalyst [32]. In the Ag/AgCl/TiO<sub>2</sub> [30] system, it is considered that the photocatalysts are of high activity for the Ag/AgCl nanoparticles absorb the photon, which is beneficial to the separation of electron and hole, and thus increases the photocatalytic activity of the semiconductor. There are articles on the metal doped ZnO [29,33] with the same conclusion that the improved activity is mainly due to the better charge separation ability. In the Ag/AgCl/ZnO catalyst, Ag/AgCl can be used as effective electron scavengers to trap the

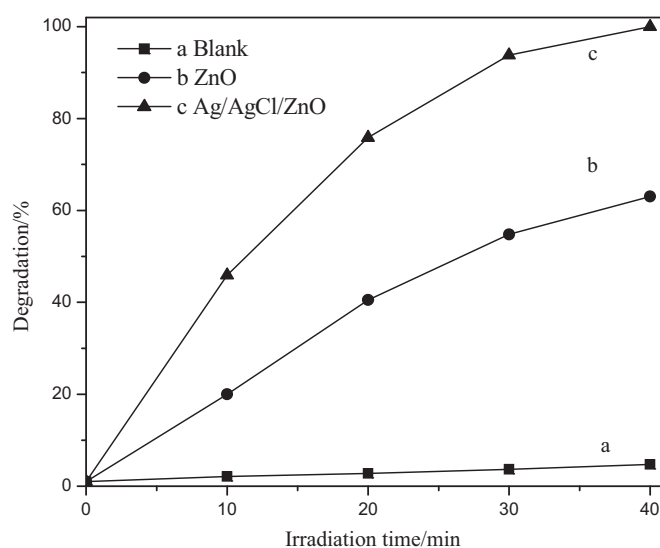
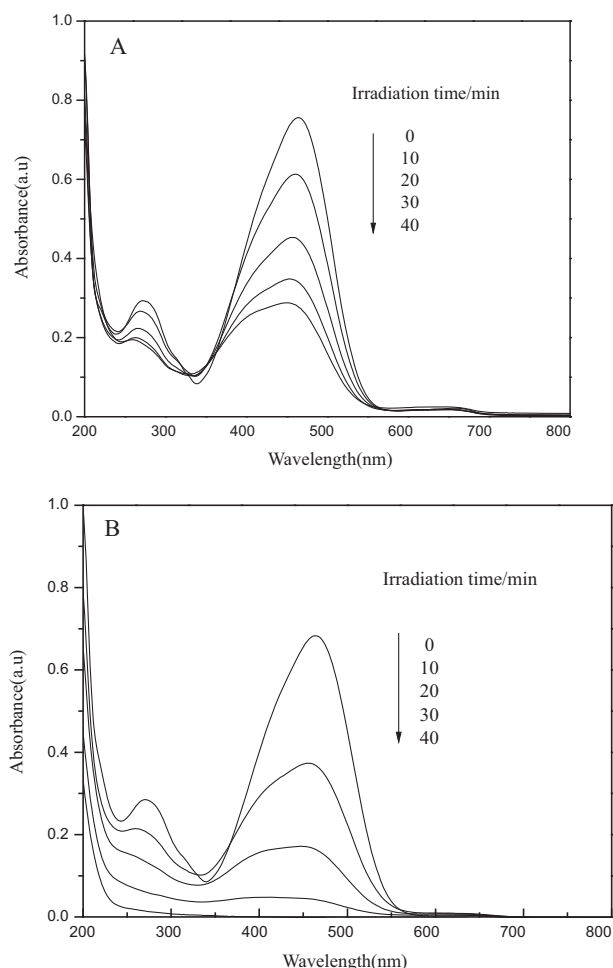


Fig. 6. Photocatalytic degradation of MO (a) without photocatalyst (b) with ZnO (c) with Ag/AgCl/ZnO.





**Fig. 7.** Absorption spectral changes of MO under UV light irradiation by ZnO (A) and Ag/AgCl/ZnO (B). [ZnO] = 0.5 g/L; [Ag/AgCl/ZnO] = 0.5 g/L; [MO] = 10 mg/L.

electron, and then the photocatalytic activity can be enhanced. The temporal evolution of the absorption spectral changes during the photocatalytic degradation of MO by the pure ZnO and Ag/AgCl/ZnO are shown in Fig. 7. It is found that the absorption peak of the solution decreases slowly in the case of ZnO sample (Fig. 7A). By contrast, in the presence of Ag/AgCl/ZnO catalyst (Fig. 7B), it shows a faster decrease in the absorbance of MO solution. The color of the suspension changed to colorless after 40 min, which indicates that the MO molecular was indeed decomposed in the reaction process.

### 3.6. The repeated experiment and the photocatalytic mechanism

The repeated experiment of the sample is conducted through the degradation of MO, as shown in Fig. 8. It is found that after five recycles, the degradation rate is not significantly decreased, which indicates that the catalytic activity of the catalysts keep stable during the process. It can be seen that the activity slightly decreases after the first cycle, which is probably due to the drop of a small amount of Ag/AgCl particles from the walls of ZnO. Then the activity nearly keeps the same value. However, the XRD of the samples used for different consecutive photooxidation experiments with MO solution (shown in Fig. 9) show that the intensity of metal Ag becomes stronger during the reaction, while the AgCl phase disappears in the sample after 28-time recycled experiments. It suggests that the AgCl gradually changes into  $\text{Ag}^0$  during the reaction. Although the constitution of the samples has been changed,

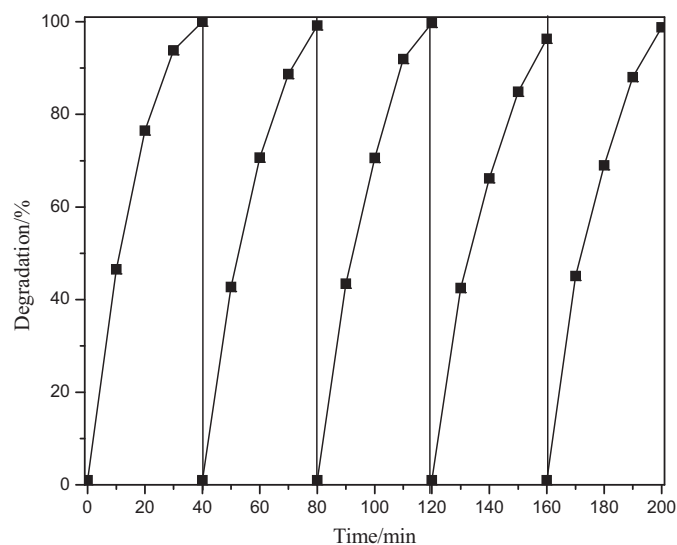


**Fig. 8.** Photocatalytic degradation curve of Ag/AgCl/ZnO composite under UV-light irradiation for five consecutive cycles.

the activity of the samples does not change evidently after the recycled experiment.

In order to confirm the junction structure of the sample after 28-time recycling, the catalyst was investigated by HRTEM, as shown in Fig. 10. The HRTEM image in Fig. 10a shows that the cocatalyst metal Ag with nice particle deposits on the ZnO surface. The magnified HRTEM image in Fig. 10b exhibits fringes with lattice spacing of ca. 0.1179 nm and 0.1477 nm, which correspond to the (2 2 2) plane of metal Ag and the (1 0 3) plane of ZnO, respectively. The result indicates that the Ag/AgCl/ZnO structure has changed to Ag/ZnO after 28 times recycled experiments. The intimate contact between Ag and ZnO favors the formation of junctions between the two components, so the photocatalytic activity of the sample keeps high.

It is very interesting that the photocatalyst changes in this system, but does not change in other systems. Besides, the photocatalyst changes, but the photocatalytic activity does not change.

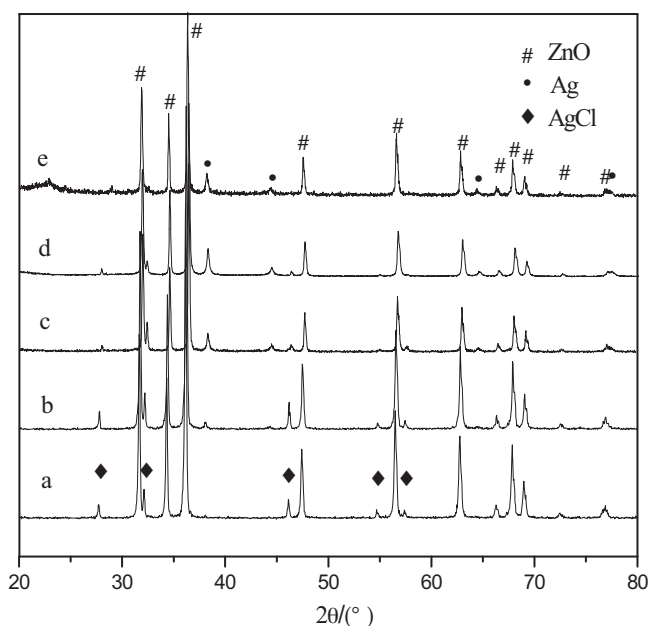


**Fig. 9.** The XRD of (a) The as-prepared Ag/AgCl/ZnO, (b) 1-time recycled sample, (c) 5-time recycled sample, (d) 9-time recycled sample, (e) 28-time recycled sample.

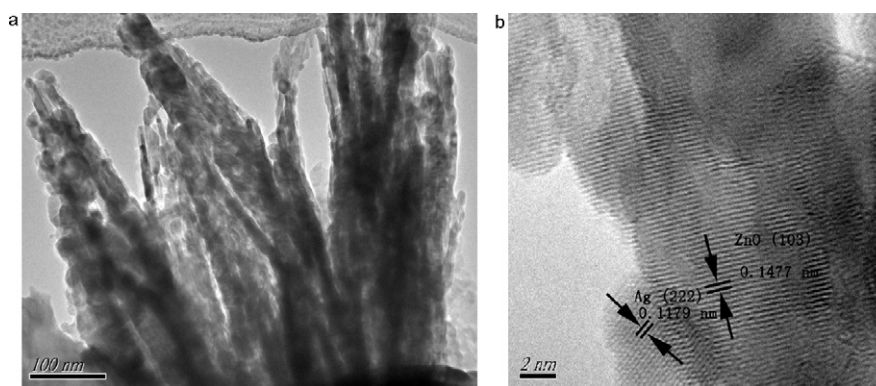


Fig. 10. (a) TEM image of the 28-time recycled sample, (b) HRTEM images of the sample.

Therefore, it is necessary to investigate the photocatalytic mechanism of the sample. The possible mechanistic pathway of the catalysts for photocatalytic degradation of MO is proposed as follows, as shown in Fig. 11: Firstly, under UV light irradiation, photo-generated electron-hole pairs ( $e_{cb}^- - h_{vb}^+$ ) were formed in ZnO NPs (Eq. (1), Fig. 11 I). Secondly, Ag nanoparticles on the surface of the ZnO absorbed UV light, and generated  $Ag^+$  and  $e^-$  (Eq. (2), Fig. 11 II). The  $e_{cb}^-$  reacted with  $Ag^+$  to form Ag (Eq. (3)), and the  $e^-$  from Eq. (2) and the other  $e_{cb}^-$  were expected to be trapped by  $O_2$  molecules in solution. Then it could form superoxide ions ( $\cdot O_2^-$ ) and other oxygen species (Eqs. (4)–(6), Fig. 11 II and III) [34,35]. The generated radicals reacted with organic pollutant (Eq. (7)). Thirdly, the  $h_{vb}^+$  could react with AgCl [24] to form  $Ag^+$  and  $Cl^0$  (Eq. (8), Fig. 11 IV), and a part of  $h_{vb}^+$  generated by ZnO reacted with  $OH^-$  to form  $\cdot OH$  (Eq. (9)) [30]. The  $Cl^0$  and  $\cdot OH$  could react with the MO organic pollutant (Eqs. (10) and (11), Fig. 11 V). Lastly,  $Ag^+$  was combined with  $Cl^-$  to form AgCl back (Eq. (12), Fig. 11 VI). As some of  $Ag^+$  was reduced to Ag by  $e_{cb}^-$ , a few of  $Cl^-$  could not be combined with  $Ag^+$  to form AgCl. So the  $Cl^-$  generated in the decoloring reaction was poured during the repeated experiment. Compared with Ag/AgCl/TiO<sub>2</sub> [36], Ag/AgBr/WO<sub>3</sub>·H<sub>2</sub>O [26] systems, the Ag/AgCl/ZnO structure was unstable, because ZnO was excited by the light and hence generated chain reactions to complete the conversion of Ag/AgCl/ZnO  $\rightarrow$  Ag/ZnO. The emphasis of this study is to investigate the change of the catalyst, which is different from other catalysts.

The reaction mechanism of the ZnO-based catalyst was also different from the pure Ag/AgCl [24] structure. The pure Ag/AgCl could

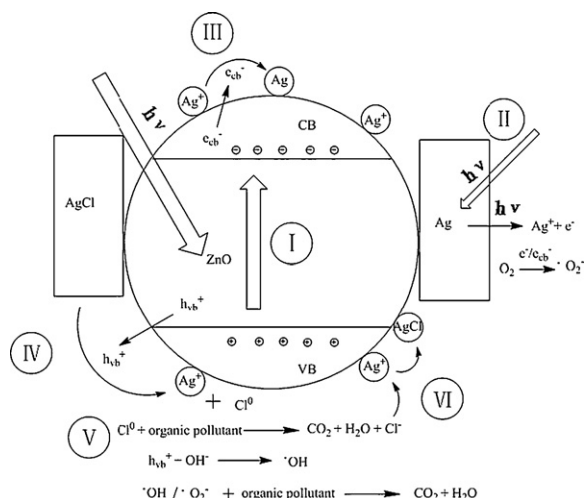
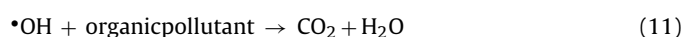
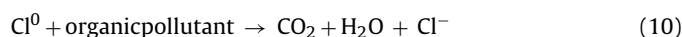
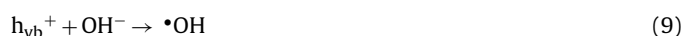
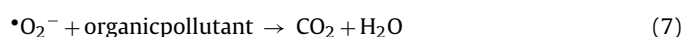
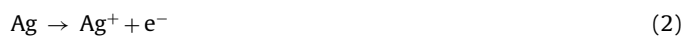


Fig. 11. The proposed reaction mechanism of the system.

be stable after several cycle reactions, because all the  $Cl^-$  could be combined with  $Ag^+$ . But in the case of Ag/AgCl/ZnO system, part of the  $Ag^+$  could be combined with  $e_{cb}^-$  generated from ZnO. In this case, some  $Cl^-$  could not be combined with  $Ag^+$  to form AgCl because of the insufficient amount of  $Ag^+$ . Therefore, it led to the change of the catalyst in the reaction process.

In order to support the opinion that  $e_{cb}^-$  also reacted with  $Ag^+$  from Eq. (3), AgCl/ZnO has been synthesized. The XRD of the AgCl/ZnO and AgCl/ZnO used after 8-time recycling have been analyzed. It is clear that after 8 recycling times, the AgCl/ZnO also changes into Ag/AgCl/ZnO (The XRD is not shown here). The conversion of AgCl/ZnO  $\rightarrow$  Ag/AgCl/ZnO indicates that  $e_{cb}^-$  also reacted with  $Ag^+$  from Eq. (3).



#### 4. Conclusions

The new composite Ag/AgCl/ZnO was synthesized through a two-step hydrothermal synthesis route. It was clearly demonstrated that Ag/AgCl/ZnO exhibited much better catalytic activity than the pure ZnO in the MO solution. Interestingly, it was found that the construction of the catalyst changed during the reaction, but the catalytic activity of the sample almost kept the same under the repeated experiments. The degradation efficiency of the sample could still keep at 98% in 40 min after 5-time recycles. Ag/AgCl enhanced the charge separation ability of the photocatalyst, and inhibited the photocorrosion of ZnO. So the photocatalytic ability of ZnO could keep stable, and its crystal could keep stable after several recycled experiments. In the reaction process, the ZnO was excited by the UV light, and the  $e_{cb}^-$  generated from ZnO was combined with part of the  $Ag^+$ . Therefore, some  $Cl^-$  could not be combined with  $Ag^+$  to form AgCl, which led to the conversion of

Ag/AgCl/ZnO  $\rightarrow$  Ag/ZnO in the reaction process. And the results of the XRD, XPS are in accordance with the proposed mechanism. Ag/AgCl/ZnO also shows activity in degradation of other organic dyes, such as Methylene Blue (MB), Rhodamine B (RhB). Besides environmental application, it is expected that the synthesized Ag/AgCl/ZnO may have potential application in the other fields.

## Acknowledgements

The authors genuinely appreciate the financial support of this work from the National Nature Science Foundation of China (No. 21007021, 21076099 and 20876071) and Research Foundation of Jiangsu University (10JDG128), Society Development Fund of Zhenjiang (SH2010006) and Doctoral Innovation Fund of Jiangsu (CX10B-275Z).

## References

- [1] T. Nakashima, N. Kimizuka, *J. Am. Chem. Soc.* 125 (2003) 6386–6387.
- [2] A. Azam, F. Ahmed, N. Arshi, M. Chaman, A.H. Naqvi, *J. Alloys Compd.* 496 (2010) 399–402.
- [3] J.Z. Su, L.J. Guo, S. Yoriya, C.A. Grimes, *Cryst. Growth Des.* 10 (2010) 856–861.
- [4] G.Q. Li, S.C. Yan, Z.Q. Wang, X.Y. Wang, Z.S. Li, J.H. Ye, Z.G. Zou, *Dalton. Trans.* 40 (2009) 8519–8524.
- [5] G.L. Huang, C. Zhang, Y.F. Zhu, *J. Alloys Compd.* 432 (2007) 269–276.
- [6] L. Shen, Z.Q. Ma, C. Shen, F. Li, B. He, F. Xu, *Superlattices Microstruct.* 48 (2010) 426–433.
- [7] L.M. Wu, F.F. Song, X.X. Fang, Z.X. Guo, S. Liang, *Nanotechnology* 21 (2010) 475502.
- [8] Y. Shen, T. Yamazaki, Z.F. Liu, D. Meng, T. Kikuta, *J. Alloys Compd.* 488 (2009) L21–L25.
- [9] J.J. Gu, L.H. Liu, H.T. Li, Q. Xu, H.Y. Sun, *J. Alloys Compd.* 508 (2010) 516–519.
- [10] P. Huang, X. Zhang, J.M. Wei, B.X. Feng, *J. Alloys Compd.* 489 (2010) 614–619.
- [11] U.I. Gaya, A.H. Abdullah, M.Z. Hussein, Z. Zainal, *Desalination* 263 (2010) 176–182.
- [12] S. Sakthivel, B. Neppolian, M.V. Shankar, B. Arabindoo, M. Palanichamy, V. Murugesan, *Sol. Energy Mater. Sol. Cells* 77 (2003) 65–82.
- [13] L.W. Zhang, H.Y. Cheng, R.L. Zong, Y.F. Zhu, *J. Phys. Chem. C* 113 (2009) 2368–2374.
- [14] L. Wang, L.X. Chang, B. Zhao, Z.Y. Yuan, G.S. Shao, W.J. Zheng, *Inorg. Chem.* 47 (2008) 1443–1452.
- [15] Z.Y. Wang, B.B. Huang, Y. Dai, X.Y. Qin, X.Y. Zhang, P. Wang, H.X. Liu, J.X. Yu, *J. Phys. Chem. C* 113 (2009) 4612–4617.
- [16] S.F. Chen, W. Zhao, W. Liu, S.J. Zhang, *Appl. Surf. Sci.* 255 (2008) 2478–2484.
- [17] R.L. Liu, Y.X. Huang, A.H. Xiao, H.Q. Liu, *J. Alloys Compd.* 503 (2010) 103–110.
- [18] C. Xu, L.X. Cao, G. Su, W. Liu, X.F. Qu, Y.Q. Yu, *J. Alloys Compd.* 497 (2010) 373–376.
- [19] T.K. Jia, W.M. Wang, F. Long, Z.Y. Fu, H. Wang, Q.J. Zhang, *J. Alloys Compd.* 484 (2009) 410–415.
- [20] J. Xu, Y.G. Chang, Y.Y. Zhang, S.Y. Ma, Y. Qu, C.T. Xu, *Appl. Surf. Sci.* 255 (2008) 1996–1999.
- [21] C.L. Ren, B.F. Yang, M. Wu, J. Xu, Z.P. Fu, Y. Lv, T. Guo, Y.X. Zhao, C.Q. Zhu, *J. Hazard. Mater.* 182 (2010) 123–129.
- [22] C. Karunakaran, V. Rajeswari, P. Gomathisankar, *J. Alloys Compd.* 508 (2010) 587–591.
- [23] C.H. An, S. Peng, Y.G. Sun, *Adv. Mater.* 22 (2010) 2570–2574.
- [24] P. Wang, B.B. Huang, X.Y. Qin, X.Y. Zhang, Y. Dai, J.Y. Wei, M.H. Whangbo, *Angew. Chem. Int. Ed.* 47 (2008) 7931–7933.
- [25] T. Morimoto, K. Suzuki, M. Torikoshi, T. Kawahara, H. Tada, *Chem. Commun.* (2007) 4291–4293.
- [26] P. Wang, B.B. Huang, X.Y. Qin, X.Y. Zhang, Y. Dai, M.H. Whangbo, *Inorg. Chem.* 48 (2009) 10697–10702.
- [27] H. Xu, H.M. Li, C.D. Wu, J.Y. Chu, Y.S. Yan, H.M. Shu, Z. Gu, *J. Hazard. Mater.* 153 (2008) 877–884.
- [28] Y.H. Zheng, L.R. Zheng, Y.Y. Zhan, X.Y. Lin, Q. Zheng, K.M. Wei, *Inorg. Chem.* 46 (2007) 6980–6986.
- [29] D.D. Lin, H. Wu, R. Zhang, W. Pan, *Chem. Mater.* 21 (2009) 3479–3484.
- [30] W.W. Lu, S.Y. Gao, J.J. Wang, *J. Phys. Chem. C* 112 (2008) 16792–16800.
- [31] S.C. Zhang, C.A. Zhang, Y. Man, Y.F. Zhu, *J. Solid State Chem.* 179 (2006) 62–69.
- [32] M.L. Zhang, T.C. An, X.L. Liu, X.H. Hu, G.Y. Sheng, J.M. Fu, *Mater. Lett.* 64 (2010) 1883–1886.
- [33] C.D. Gu, C. Cheng, H.Y. Huang, T.L. Wong, N. Wang, T.Y. Zhang, *Cryst. Growth Des.* 9 (2009) 3278–3285.
- [34] H.C. Yatmaz, A. Akyol, M. Bayramoglu, *Ind. Eng. Chem. Res.* 43 (2004) 6035–6039.
- [35] J.G. Yu, J.F. Xiong, B. Cheng, S.W. Liu, *Appl. Catal. B: Environ.* 60 (2005) 211–221.
- [36] J.G. Yu, G.P. Dai, B.B. Huang, *J. Phys. Chem. C* 113 (2009) 16394–16401.